ELSEVIER

Journal of Crystal Growth 187 (1998) 234–239

JOURNAL OF CRYSTAL GROWTH

Metalorganic vapor phase epitaxy of manganese gallide thin films and growth temperature dependence of its crystal structure

M. Ishii*,[1], S. Iwai, T. Ueki, Y. Aoyagi

The Institute of Physical and Chemical Research (RIKEN), Hirosawa 2-1, Wako-shi, Saitama 351-01, Japan

Received 2 June 1997; accepted 13 October 1997

Abstract

The metalorganic vapor phase epitaxy (MOVPE) is adopted for the manganese gallide (Mn_xGa_y) thin film growth on AlP/GaP heterostructures for the first time. Tricarbonylmethylcyclopentadienyl manganese (TCM) and trimethylgallium (TMG) are used as metalorganic gas sources for Mn and Ga elements, respectively. The Mn_xGa_y crystal structure depends on the growth temperature condition; while the γ-brass-type cubic Mn_8Ga_5(1 0 0) crystal is grown below the growth temperature of 620°C, the hexagonal $Mn_3Ga(1\,0\,\bar{1}\,0)$ is obtained above this temperature.

PACS: 42.70. −a; 75.50; 81.15.Kk; 81.30

Keywords: MOVPE; TCM; TMG; Mn_8Ga_5; Mn_3Ga; Phase diagram

1. Introduction

The crystal growth of various 3d transition metals and their compounds on semiconductors such as GaAs has been extensively investigated [1–4] because the epitaxial thin films of these materials are not only important for simple magnetic applications such as memory devices but also for new magneto-optic devices with hybrid structures of the magnetic material and the compound semiconductor. Manganese (Mn) easily makes compounds with group-III or -V materials, which are well-known elements of compound semiconductors, resulting in magnetic binary compounds such as δ-$Mn_{1-x}Ga_x$ ($x = 0.5$–0.7) [5,6], τ-MnAl [4,7,8] and MnAs [9,10]. The heteroepitaxial growth of these Mn compounds have been performed using the conventional molecular beam epitaxy (MBE) system with a Mn source.

*Corresponding author.

[1]Present address: Japan Synchrotron Radiation Research Institute (JASRI), Spring-8, Kamigori, Ako-gun, Hyogo 678-12, Japan. Fax: + 81 7915 8 0830; e-mail: ishiim@sp8sun.spring8.or.jp.

0022-0248/98/$19.00
PII S0022-0248(97)00876-2

Recently, we pointed out that a high-performance X-ray mirror might be fabricated as manganese gallide (Mn_xGa_y)/AlP single crystal multilayer structures [11]. In particular, the Mn_xGa_y/AlP multilayer with a periodic length of a few monolayers (MLs) is expected to function as an X-ray mirror in the wavelength region of 2–4 nm. This X-ray wavelength region is well known as the 'water window' which is important for biological applications such as X-ray microscopy. In order to fabricate the X-ray multilayer mirror, high- and low-density materials with low X-ray absorption are alternatively deposited as spacer and scatter layers, respectively. In addition to the favorable property of the relatively high density of Mn_xGa_y, X-ray loss in the Mn_xGa_y scatter layer is expected to be low in this water window due to the MnL absorption edge at $\sim$1.9 nm. This new application for Mn_xGa_y/AlP provides the opportunity for the realization of an active X-ray mirror with electric and magnetic properties.

In addition to this new application of Mn_xGa_y/AlP X-ray mirror, a magnetic coupling device with a δ-$Mn_{1-x}Ga_x$/GaAs/δ-$Mn_{1-x}Ga_x$ of trilayer has also been investigated recently [12]. The Mn_xGa_y/semiconductor multilayer will be more important for new device fabrications. In order to realize well-defined short periodic multilayer structures, the establishment of a Mn_xGa_y thin film growth technique is necessary. However, there are only a few reports on the crystal growth of Mn_xGa_y thin films at this time. In all these reports, δ-$Mn_{1-x}Ga_x$ thin films are grown by the template method in the MBE system [6,7]. In that method, a two-step crystallization procedure is adopted: amorphous template formation by the alternatively supplying Mn and Ga sources at room temperature, followed by crystallization by annealing at $\sim$200°C. This method, in which the temperature is controlled during the growth, is unsuitable for multilayer formations. Moreover, though Mn_xGa_y has numerous crystal structure phases with different magnetic properties [13–16], the thin film growth of Mn_xGa_y crystals other than δ-$Mn_{1-x}Ga_x$ has never been discussed.

In this study, metalorganic vapor phase epitaxy (MOVPE) of Mn_xGa_y is performed for the first time. This MOVPE is achieved by the direct crystal growth method without the predeposition of an amorphous template. The phase transition of the Mn_xGa_y crystal structure is also discussed by means of growth temperature and source gas flow rate selection.

2. Experimental procedure

An experimental apparatus for the Mn_xGa_y MOVPE is shown in Fig. 1. It has a cold-wall-type horizontal quartz reactor with a RF heating system. The substrates were mounted on a carbon susceptor. The metalorganic source gases for Mn and Ga elements were tricarbonylmethylcyclopentadienyl manganese (TCM) and trimethylgallium (TMG), respectively. TCM is a liquid at room temperature (melting point = 1.5°C) with a relatively high vapor pressure of 0.05 Torr at 20°C [17,18]. In our MOVPE system, these metalorganic gases were introduced into the reactor by H_2 bubbling. The TCM and TMG liquid gas sources were kept at 40 and -10°C, respectively. The H_2 flow rate through TCM was varied between 0 and 560 sccm. Hydrogen carrier gas was continuously introduced, and the total gas pressure in the reactor was fixed at 20 Torr. The substrates were (1 0 0)-oriented non-doped GaP which were chemically etched in $HCl : HNO_3 : H_2O = 2 : 1 : 2$ solution at 55°C for 2 min and then dipped in $(NH_4)_2S_x$ at room temperature for 10 min. Immediately after rinsing with methanol to remove excess $(NH_4)_2S_x$ on the surface, the substrates were introduced into the reactor. This $(NH_4)_2S_x$ treatment improves the surface

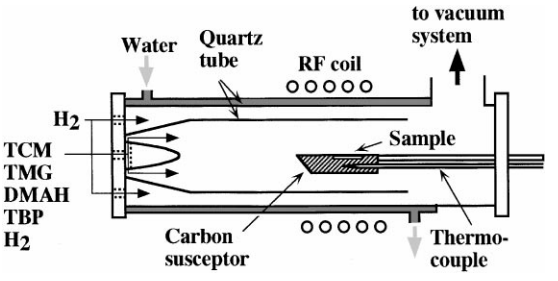

Fig. 1. The experimental apparatus for Mn_xGa_y MOVPE. It is comprised of a cold-wall-type horizontal quartz reactor with a RF heating system.

morphology and prevents the oxidation of GaP by sulfur termination of surface atoms [19,20]. The sulfur on the substrate was removed by annealing in H_2 ambient at 460°C for 30 min. Prior to Mn_xGa_y deposition, a GaP buffer layer of ~0.1 μm and the following AlP thin film of ~50 nm were grown by conventional MOVPE at 700°C. In the growth of these buffer layers, TMG and dimethylaluminum hydride (DMAH) were used as the source gases of group-III elements. The group-V source was tertiarybutylphosphine (TBP). Mn_xGa_y growth on the AlP/GaP heterostructure is attempted as a first step towards the fabrication of Mn_xGa_y/AlP multilayers. After the AlP/GaP heterostructure formation, the substrate temperature was set at the Mn_xGa_y growth temperature in the TBP ambient. The substrate temperature was varied between 400 and 700°C. After a 2 s interruption of TBP feeding, Mn_xGa_y was grown by simultaneously introducing TMG and TCM into the reactor.

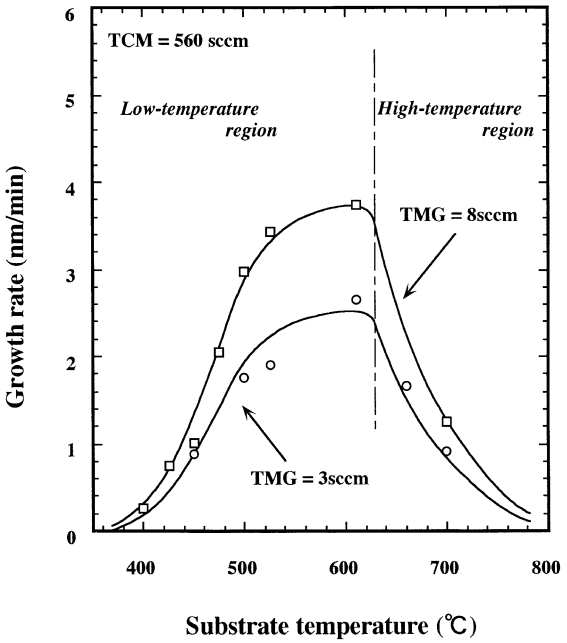

Fig. 2. The substrate temperature dependence of the Mn_xGa_y growth rate. The TMG flow rates were 8 (open squares) and 3 sccm (open circles).

3. Results and discussion

Fig. 2 shows the substrate temperature dependence of the Mn_xGa_y growth rate. In this experiment, the flow rate of TCM was fixed at 560 sccm. The TMG flow rates were 8 (open squares) and 3 sccm (open circles). Scanning electron microscopy (SEM) confirmed that a mirror-like surface is presented after the growth. As shown in this figure, the temperature dependence is similar for high and low TMG flow rates. Mn_xGa_y growth is observed above a substrate temperature of ~400°C, and the growth rate increases with increasing temperature. This minimum growth temperature of Mn_xGa_y corresponds to that of MnAs MOVPE using TCM and AsH_3, as reported by Lane et al. [21]. In the MnAs case, it was concluded that this minimum temperature is equal to the TCM thermal decomposition temperature. In our Mn_xGa_y growth, the TMG decomposition must be considered. The TMG decomposition temperature in H_2 ambient is ~400°C [22] which is the same as that of TCM [23], indicating that this minimum growth temperature of Mn_xGa_y is caused by the decomposition of both TCM and TMG. The growth rate has a peak at ~620°C, and rapidly decreases above this temperature, independent of the TMG flow rate. For the sake of convenience, the growth temperature regions below and above this peak temperature are defined as the 'low-temperature region' and the 'high-temperature region', respectively. In order to identify the crystal structure in both the low- and high-temperature regions, Cu K_α X-ray diffraction measurements were performed.

Fig. 3 shows typical X-ray diffraction patterns of samples grown in (a) the low-temperature region and (b) the high-temperature region. The film thickness was ~60 nm. As indicated in Fig. 3a, Mn_8Ga_5(3 0 0) and higher order index peaks are observed; no other peaks are detected. This result indicates that (1 0 0)-oriented γ-brass-type cubic Mn_8Ga_5 with the lattice constant of 0.8992 nm [14] is grown on AlP/GaP in this temperature region. In contrast, hexagonal Mn_3Ga(2 0 0) and (4 0 0) peaks are observed in Fig. 3b, and X-ray diffraction peaks from the cubic Mn_8Ga_5 are not obtained. In the high-temperature region, (1 0 $\bar{1}$ 0) oriented hexagonal Mn_3Ga with the lattice parameters $a = 0.5406$ nm and $c = 0.4360$ nm [15,16] is

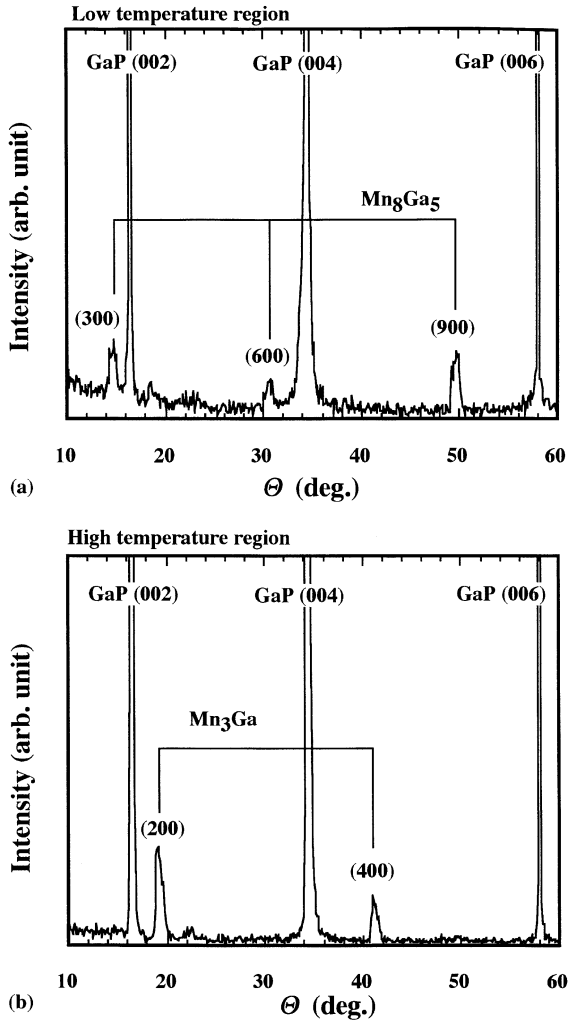

Fig. 3. Typical X-ray diffraction patterns of samples grown in (a) the low-temperature region and (b) the high-temperature region. The (1 0 0) oriented γ-brass-type cubic Mn_8Ga_5 is grown on AlP/GaP in the low-temperature region. (1 0 $\bar{1}$ 0)-oriented hexagonal Mn_3Ga is obtained in the high-temperature region.

grown. The epitaxial relationship in the film plane of these crystals is now under investigation. In other works, these crystals were prepared by melting a Mn and Ga mixture, and followed by quenching. This is the first report of the thin film growth of these crystals by MOVPE.

As shown in Fig. 2, growth rate decreases with increasing growth temperature in the high-temperature region. A similar characteristic was observed

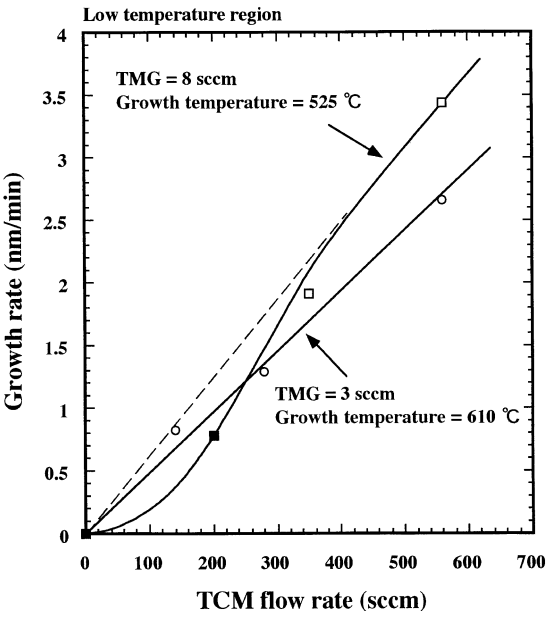

Fig. 4. The TCM flow rate dependence of Mn_8Ga_5 in the low-temperature region.

in polycrystalline MnAs MOVPE using TCM, in which the growth rate has a peak at 475°C. These results suggest that the reduction of the growth rate at high temperature is mainly due to the intrinsic properties of TCM, such as adsorption and decomposition. In the Mn_xGa_y case, it is considered that the change of the adsorption property and/or the decomposition state at high temperatures results in the phase transition from cubic Mn_8Ga_5 to hexagonal Mn_3Ga.

Fig. 4 shows the TCM flow rate dependence of Mn_8Ga_5 in the low-temperature region. The TMG low rates were 3 and 8 sccm. As shown by open circles, when the TMG flow rate is 3 sccm, the growth rate has a linear dependence with respect to the TCM flow rate, at the substrate temperature of 610°C. In contrast, below the TCM flow rate of 350 sccm, the growth rate at the TMG flow rate of 8 sccm becomes lower than that expected from the linear dependence (dashed line). Especially for 200 sccm, the grown film is covered with a liquid-like amorphous material which is easily wiped off. In this figure, the open squares mean the normal growth rate of solid films, whereas the filled squares

indicate that the growth rate is evaluated from the solid film thickness after the removal of the amorphous material. The decrease of the growth rate at the TCM flow rate of 200 sccm is considered to be caused by a phase transition from the crystal to the amorphous film.

The deviation from the linear dependence is more significant in the high-temperature region, as shown in Fig. 5. In this experiment, the growth temperature was fixed at 700°C. The TMG flow rate was varied between 3 and 8 sccm. As in Fig. 4, the filled circles and squares indicate that liquid-like amorphous materials are taken away before thickness measurements. The growth rate was rapidly decreased below $\sim$500 sccm in the case of the TMG flow rate of 8 sccm. At the TCM flow rate of 280 sccm, the deposited material was completely removed, and no solid film growth was observed. This critical flow rate for the solid film growth decreased to 140 sccm at the TMG flow rate of 3 sccm. This result indicates that a phase transition from the crystal to the amorphous material occurs due to the disproportion between the feeding rate of TCM and that of TMG, and that the amorphous material is a Ga-rich alloy.

From these results, a phase diagram of the crystal structures is derived, as shown in Fig. 6. The horizontal axis indicates the TCM flow rate divided by the TMG flow rate. As discussed in Figs. 2 and 3, the crystal structures of the thin films are independent of the TMG flow rate. Hence, the phase transition from Mn_8Ga_5 to Mn_3Ga is independent of TCM/TMG flow rates. The closed circles indicate the deposition of amorphous material. At the point of TCM/TMG = 25 (=200 sccm/8 sccm) and growth temperature=525°C, the amorphous material and the crystal mixture are grown as discussed for Fig. 4; this point is on the boundary of the transition between crystal and amorphous deposition.

As shown in this phase diagram, δ-$Mn_{1-x}Ga_x$ which can be grown by the template method is not obtained in these experimental conditions. The crystallization temperature of δ-$Mn_{1-x}Ga_x$ is lower than the MOVPE growth temperature, suggesting that δ-$Mn_{1-x}Ga_x$ is unstable at high temperature. The structural stability of Mn_8Ga_5 and Mn_3Ga might be a reason for the direct epitaxial growth without the amorphous template. On the other hand, since Mn is considered to be reactive to Al and P at high temperature, further study on the interface diffusion in MOVPE grown films is

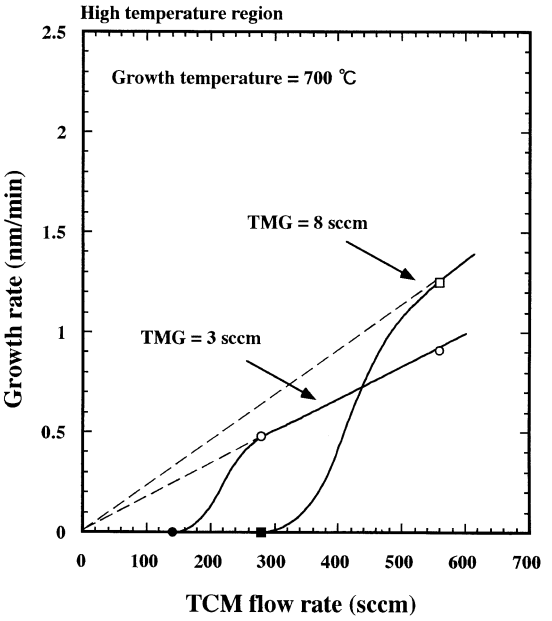

Fig. 5. The TCM flow rate dependence of Mn_3Ga in the high temperature region. The deviation from the linear dependence is more significant than that in the low-temperature region.

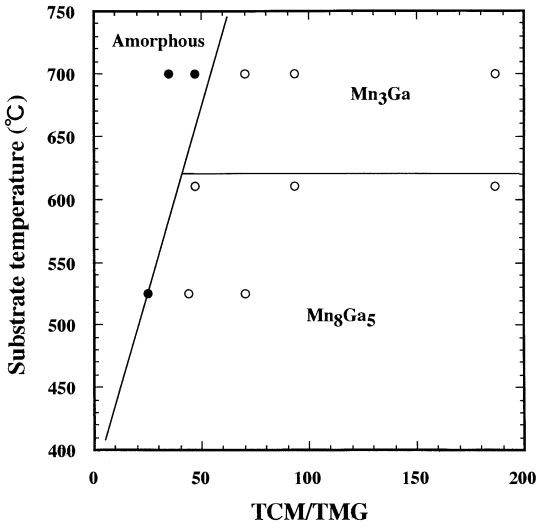

Fig. 6. The phase diagram of the Mn_xGa_y crystal structures.

necessary for fabrication of the semiconductor/Mn_xGa_y multilayer structure.

4. Summary

Mn_xGa_y thin films were grown by metalorganic vapor phase epitaxy (MOVPE) using tricarbonylmethylcyclopentadienyl manganese (TCM) and trimethylgallium (TMG). The (1 0 0)-oriented γ-brass-type cubic Mn_8Ga_5 was grown below the growth temperature of 620°C. On the other hand, the (1 0 $\bar{1}$ 0)-oriented hexagonal Mn_3Ga was obtained above this temperature. These results indicate that crystal structures with different magnetic properties can be obtained by selection of the growth temperature. The phase transition from the crystal to the amorphous Ga-rich alloy was also observed under the condition of the disproportionate flow rates of TCM and TMG. The phase diagram of crystal structure has been summarized.

Acknowledgements

This work was supported in part by a Grant-in-Aid for Exploratory Research from the Ministry of Education, Science, Sports and Culture.

References

[1] R. Kaplan, N. Bottka, Appl. Phys. Lett. 41 (1982) 972.
[2] G.A. Prinz, Phys. Rev. Lett. 54 (1985) 1051.
[3] J.A. Wolf, J.J. Krebs, Y.U. Idzerda, G.A. Prinz, J. Appl. Phys. 76 (1994) 6452.
[4] T.L. Cheeks, J.P. Harbison, M. Tanaka, D.M. Hwang, T. Sands, V.G. Keramidas, J. Appl. Phys. 75 (1994) 6665.
[5] K.M. Krishnan, Appl. Phys. Lett. 61 (1992) 2365.
[6] M. Tanaka, J.P. Harbison, J. DeBoeck, T. Sands, B. Philips, T.L. Cheeks, V.G. Keramidas, Appl. Phys. Lett. 62 (1993) 1565.
[7] T. Sandas, J.P. Harbison, M.L. Leadbeater, J. Allen, G.W. Hull, R. Ramesh, V.G. Keramidas, Appl. Phys. Lett. 57 (1990) 2609.
[8] J.P. Harbison, T. Sands, R. Ramesh, L.T. Florez, B.J. Wilkens, V.G. Karemidas, J. Crystal Growth 111 (1991) 978.
[9] M. Tanaka, J.P. Harbison, T. Sands, T.L. Cheeks, V.G. Karamidas, J. Vac. Sci. Technol. B 12 (1994) 1091.
[10] K. Akeura, M. Tanaka, K. Ueki, T. Nishinaga, Appl. Phys. Lett. 67 (1995) 3349.
[11] M. Ishii, S. Iwai, H. Kawata, T. Ueki, Y. Aoyagi, J. Crystal Growth 180 (1997) 15.
[12] W. Van Roy, H. Akinaga, S. Miyanishi, K. Tanaka, Appl. Phys. Lett. 69 (1996) 711.
[13] T.A. Bither, W.H. Cloud, J. Appl. Phys. 36 (1965) 1501.
[14] I. Tsuboya, M. Sugihara, J. Phys. Soc. Japan 18 (1963) 1096.
[15] I. Tsuboya, M. Sugihara, J. Phys. Soc. Japan 18 (1963) 143.
[16] H. Niida, T. Hori, Y. Nakagawa, J. Phys. Soc. Japan 32 (1983) 1512.
[17] P.J. Wright, B. Cockayne, A.F. Cattell, P.J. Dean, A.D. Pitt, J. Crystal Growth 59 (1982) 155.
[18] A. Nouhi, R.J. Stirn, Appl. Phys. Lett. 51 (1987) 2251.
[19] A. Wakahara, X.-L. Wang, A. Sasaki, J. Crystal Growth 124 (1992) 118.
[20] X.-L. Wang, A. Wakahara, A. Sasaki, Appl. Phys. Lett. 65 (1994) 2096.
[21] P.A. Lane, B. Cockayne, P.J. Wright, P.E. Oliver, M.E.G. Tilsley, N.A. Smith, I.R. Harris, J. Crystal Growth 143 (1994) 237.
[22] M. Yoshida, H. Watanabe, F. Uesugi, J. Electrochem. Soc. 132 (1985) 677.
[23] S. Wen-bin, K. Durose, A.W. Brinkman, J. Woods, J. Crystal Growth 113 (1991) 1.